Jundishapur J Nat Pharm Prod. 2026 May; 21(2): e165982 https://doi.org/10.5812/jjnpp-165982

Published Online: 2026 July 13 **Research Article**

Preparation and Characterization of Silymarin-Loaded Nanostructured Lipid Carriers for UV-Protection

Negin Amelian [1, 2], Azadeh Ghaffari [1, 2], Azade Taheri [3], Morteza Abazari [4], Samineh Jafari [5, *]

[1] Zanjan Pharmaceutical Nanotechnology Research Center, Zanjan University of Medical Sciences, Zanjan, Iran
[2] Department of Pharmaceutical Nanotechnology, School of Pharmacy, Zanjan University of Medical Sciences, Zanjan, Iran
[3] Department of Pharmaceutics, Novel Drug Delivery Systems Research Center, Faculty of Pharmacy, Isfahan University of Medical Sciences, Isfahan, Iran
[4] Experimental and Applied Pharmaceutical Sciences Research Center, Urmia University of Medical Sciences, Urmia, Iran
[5] Department of Pharmacognosy, School of Pharmacy, Zanjan University of Medical Sciences, Zanjan, Iran

[*] ***Corresponding Author:*** Department of Pharmacognosy, School of Pharmacy, Zanjan University of Medical Sciences, Zanjan, Iran. Email: jafari_s@zums.ac.ir

Received: 31 August, 2025; **Revised:** 1 July, 2026; **Accepted:** 8 July, 2026

Abstract

Background: Silymarin is a polyphenol-rich plant extract with antioxidant and UV-absorbing properties. However, its limited solubility and stability present challenges, necessitating further formulation research.

Objectives: This study aimed to develop a novel silymarin-loaded nanostructured lipid carrier (NLC) and evaluate its in vitro photoprotective potential.

Methods: NLCs were prepared by melt emulsification followed by high-shear homogenization using cetyl palmitate (CP) or beeswax (BW) as the solid lipids, oleic acid as the liquid lipid, and Tween 80 as the surfactant. The NLCs were characterized in terms of particle size, polydispersity index, zeta potential, drug loading, and entrapment efficiency. Their infrared spectra, thermal behavior, crystallinity, in vitro drug release, rheological properties, and in vitro sun protection effects were also evaluated. In addition, a stability study was conducted on the BW-containing NLCs.

Results: Formulations containing CP showed mean particle sizes ranging from 102.9 to 140.0 nm and a polydispersity index (PDI) of 0.25 - 0.48, whereas those incorporating BW showed a broader size range (108.8 - 898.8 nm; PDI: 0.28 - 0.88). The developed silymarin-loaded NLCs exhibited high encapsulation efficiency, as confirmed by DSC, XRD, and FTIR analyses. Although silymarin-loaded NLCs, particularly BW-based formulations, exhibited relatively higher UV protection, the achieved SPF values (3.76 - 6.01) indicate that silymarin alone is insufficient for effective clinical photoprotection. Finally, stability assessments revealed notable challenges, with high silymarin loading and elevated surfactant concentrations leading to marked particle aggregation and loss of colloidal stability (PDI reaching 1.0) after three months of storage.

Conclusions: This study developed silymarin-loaded NLCs with high loading capacity and biocompatible natural ingredients. However, the formulations showed long-term stability challenges and inadequate sun protection, necessitating the inclusion of UV filters in future research. Their practical application is also limited by the need for comprehensive biocompatibility and safety assessments. Therefore, these formulations should be considered proof-of-concept systems rather than finalized delivery systems.

Keywords: Beeswax, Cetyl Palmitate, Nanostructures, Silymarin, Sun Protection Factor

1. Background

UV-induced skin damage is a global concern and a major contributor to numerous skin disorders. UVA rays promote skin aging, dryness, and cancer by generating reactive oxygen species that can damage DNA. UVB radiation induces skin responses such as erythema and tanning and, over time, can lead to chronic conditions, including accelerated aging and skin cancer. Prolonged, unprotected exposure to UV radiation is a primary cause

How to Cite: Amelian N, Ghaffari A, Taheri A, Abazari M, Jafari S. Preparation and Characterization of Silymarin-Loaded Nanostructured Lipid Carriers for UV-Protection. Jundishapur J Nat Pharm Prod. 2026;21(2):e165982. doi: https://doi.org/10.5812/jjnpp-165982

of melanoma and nonmelanoma skin cancers (1). Sunscreen application is the main strategy for protection against harmful light exposure. Topical sunscreens are classified as organic or inorganic: inorganic ingredients reflect light, whereas organic filters absorb UV rays. There is increasing interest in natural substances with antioxidant properties that protect the skin from damage, including wrinkles and aging. Plant-derived antioxidants can mitigate cellular damage and aging. Natural agents are effective, nontoxic, and provide additional benefits, motivating research into their potential to replace or reduce conventional UV filters. In particular, herbal polyphenols exhibit significant photoprotective activity and are often incorporated into sunscreens for UV protection (2).

Silymarin, derived from *Silybum marianum* seeds, is a polyphenol-rich extract containing 70 - 80% flavonolignans, mainly silybin. It is well known for its hepatoprotective and antioxidant properties, as well as additional, although less recognized, UV-protective effects. Recent studies indicate that silymarin is a broad-spectrum photoprotectant whose polyphenols prevent UV-induced damage, photoaging, and carcinogenesis. In summary, its mechanisms of action can be categorized as follows: 1) cytoprotective effects on dermal fibroblasts against UVA irradiation, 2) elimination of oxidative stress and prevention of glutathione depletion, 3) reduction of UV-induced genotoxicity and apoptosis, 4) suppression of UV-induced inflammation, and 5) prevention of UV-induced immune dysfunction (3-5). In addition, several studies have demonstrated that silymarin and its primary constituents directly absorb UV photons (5, 6). A recent investigation by Erdogan et al. showed that *S. marianum* seed extract is a valuable ingredient in sunscreen formulations because of its strong antioxidant qualities, photostability, and ability to increase the SPF of mineral filters (7). Rencber et al. incorporated silymarin and zinc oxide into NLCs to evaluate their sun protection effectiveness. The SPF values of the formulations were recorded as 6.4, 7.5, and 8.4 (8).

Despite its benefits, the practical use of silymarin is limited by low water solubility, instability upon exposure to air and light, and potential skin irritation after topical application. Meanwhile, advances in colloidal and pharmaceutical sciences have led to the development of silymarin-based formulations designed to enhance its stability, solubility, and therapeutic effectiveness. These innovations include various solubilization technologies to improve the incorporation of silymarin into effective delivery systems (9, 10).

Nanostructured lipid carriers (NLCs) are an advanced type of solid lipid nanoparticle designed to improve drug delivery by combining solid and liquid lipids. These systems increase drug-loading capacity and reduce the initial burst release of the drug. Recently, NLCs have gained popularity as effective drug delivery systems, particularly for targeted applications via various administration routes, such as topical delivery in cosmetics and skin treatments. NLCs are also developed to overcome challenges associated with the hydrophobic nature of many active compounds (11). Moreover, NLCs improve cosmetic formulations by increasing the stability and bioavailability of active ingredients and providing strong skin hydration. In sunscreens, NLCs are commonly used because they reduce the frequency of application, prolong residence time on the skin, and improve the effectiveness of sunscreen agents via UV scattering (12). In several earlier studies, researchers designed and used silymarin-NLCs for topical application. Singh et al. formulated NLC-silymarin to inhibit cell proliferation, progression, and differentiation initiated by DMBA in mouse skin, achieving favorable results (13). They also created a silymarin-NLC gel that was more effective in treating UV-induced skin irritation in rats and inhibiting SK-MEL 2 cell growth than existing market products (10). Iqbal et al. developed a silymarin-NLC gel that provided better outcomes for skin cancer treatment than conventional silymarin gel in both ex vivo and in vivo studies (14). In their research on silymarin-NLC, Momin et al. enhanced the penetration of silymarin and its efficacy in reducing the thickness of psoriasis plaques (15).

2. Objectives

The objective of this study was to prepare silymarin-loaded NLC and evaluate its protective effects against UV radiation in vitro.

3. Methods

3.1. Materials

Silymarin was a kind gift from Goldaru Herbal Pharmaceutical Co. (Iran). BW and ethanol were purchased from Sobhan Darou Co. (Iran) and Kimia Alcohol Zanjan (Iran), respectively. Sunscreen SPF30 (Ardene Sun) was obtained from Pars Hayan Pharmaceutical Co. (Iran). Oleic acid, Tween 80, and CP were acquired from Merck (Germany).

3.2. Preliminary Studies

NLC formulations were prepared using the following components: oleic acid (liquid lipid), BW or CP (solid lipid), and Tween 80 (surfactant). Previous research on silymarin-loaded NLCs indicated that a 3:7 ratio of liquid lipid to solid lipid resulted in favorable particle characteristics and stability (13, 16-18). As shown in Table 1 and Figure 1, this ratio produced acceptable outcomes (C1 and B1-B3). In subsequent formulations, a slightly higher liquid lipid proportion (1:2 ratio) improved stability and drug loading. All formulations underwent visual inspection for miscibility and phase uniformity and were evaluated for particle size. In the initial formulations, a 1:1 ratio of total lipid to surfactant was used, yielding acceptable particle size and polydispersity at the time of preparation. Accordingly, this ratio was maintained in later formulations, while the total lipid and surfactant percentages were progressively increased to enhance drug-loading capacity. Despite suitable particle size and PDI, formulations C1 and B1-B3 were excluded from further studies because of unacceptable sedimentation. Throughout the study, increasing the percentages of both Tween 80 and the lipid mixture to 15% produced stable formulations. However, statistical analysis showed that this adjustment did not significantly change the PDI or size. Therefore, formulations B4 and C2 were loaded with silymarin at different concentrations. Unlike B4 and C2, which appeared as white colloidal dispersions when prepared, the silymarin-loaded NLCs appeared as creamy yellow semisolids.

3.3. Preparation of NLC

NLC formulations were prepared using the melt emulsification and high-shear homogenization method (11, 19). Briefly, weighed amounts of lipids (Table 1) were stirred for 10 minutes at 70 - 80°C and 400 rpm (lipid phase). Similarly, the specified amount of Tween 80 was added to distilled water and stirred for 2 minutes at 400 rpm at the same temperature. The lipid phase was then added to the aqueous phase under stirring for 20 minutes at 1000 rpm. Next, the mixtures were homogenized for 15 minutes at 14 rpm (using a Silent Crusher Heidolph homogenizer) to achieve the appropriate particle size and stability.

3.4. Preparation of Silymarin-NLC

To prepare silymarin-loaded NLCs, silymarin solutions were prepared at a concentration of 1 g/40 mL of absolute ethanol. Specified volumes (Table 1) of the solution were then gradually incorporated into the melted lipid phase. The subsequent steps were performed as described above for NLC preparation.

3.5. Determination of Particle Size and Zeta Potential

The average particle size, polydispersity index (PDI), and zeta potential of the prepared formulations were determined by dynamic light scattering (DLS) (ZetaSizer Nano-ZS; Malvern Instruments Ltd., United Kingdom) at 633 nm, 20 - 25°C, and an angle of 90°. Before measurement, formulation samples were diluted 100-fold in double-distilled water.

3.6. Drug Loading and Entrapment Efficiency

Silymarin-NLC formulations (3 mL) were transferred to centrifuge tubes fitted with an ultrafilter (Amicon Ultra-4, PLHK Ultracel-PL Membrane, 30 kDa, Millipore). Tubes were centrifuged at 4400 rpm for 10 minutes to separate the organic and aqueous phases. The filtered samples were analyzed by UV spectrophotometry at 294 nm to quantify free silymarin. Finally, the percentages of drug loading (DL) and encapsulation efficiency (EE) were calculated as follows:

$$\mathrm{EE}\,(\%) = \frac{W_a - W_s}{W_a} \times 100$$

$$\mathrm{DL}\,(\%) = \frac{W_a - W_s}{W_l} \times 100$$

where Wa, Ws, and Wl denote the amount of silymarin incorporated into the formulation, the recorded weight of the drug in the supernatant, and the weight of the added lipid, respectively (20).

3.7. FTIR Analysis

Infrared spectra were recorded using an FTIR spectrophotometer (Equinox 55 LS 101, Bruker, Germany) over a frequency range of 4000 to 500 cm^{-1}. NLC formulations were dried in a vacuum oven for one week before analysis.

3.8. DSC Analysis

For DSC analysis, only formulations containing BW (B4-B7) were evaluated because they showed greater efficacy in assessing sun protection capabilities. In addition, silymarin powder, a physical mixture of

Table 1. Composition of the Prepared NLC Formulations [a]

Formulation code	Silymarin	Beeswax	Cetyl palmitate	Oleic acid	Tween 80	Distilled water
C1	-	-	0.7	0.3	1	98
C2	-	-	10	5	15	70
C3	3	-	10	5	15	67
C4	4	-	10	5	15	66
B1	-	5.25	-	2.25	7.5	85
B2	0.7	5.25	-	2.25	7.5	84.3
B3	-	7.88	-	3.38	11.25	77.5
B4	-	10	-	5	15	70
B5	1.5	10	-	5	15	68.5
B6	3	10	-	5	15	67
B7	4	10	-	5	15	66

[a] Values are expressing as percentage.

silymarin, BW, oleic acid, and Tween 80, and a geometrical mixture of silymarin + KBr (potassium bromide) were subjected to DSC analysis after vacuum-oven drying using a DSC PL model STA 780. An empty aluminum pan was used as the reference. Samples were scanned from 25°C to 250°C at a rate of 5°C/min under an air atmosphere (20 mL/min).

3.9. X-Ray Diffraction (XRD) Analysis

XRD was used for the crystallographic investigation of silymarin, CP, BW, and silymarin-NLCs containing 3% drug (C3 and B6). Measurements were performed using a Bruker X-ray diffractometer D8 Advance (Bruker AXS, Germany) by scanning 2θ in the range of 10° to 80° at a scan speed of 0.15°/minute.

3.10. Rheological Properties of NLCs

The rheological properties of the formulations and a commercial sunscreen product (Sunscreen cream SPF30, Ardene Sun) were evaluated using the cone-and-plate method (Brookfield R/S-CPS+ Rheometer, M/01 - 213-A0706 Rheometer Series, Rheo2000 software, 11 Commerce Boulevard, Middleboro, MA 02346, USA). All measurements were performed at 25°C, starting at a shear rate of 1 s^{-1} up to a maximum of 300 s^{-1}, with a measurement point duration of 10 seconds.

3.11. In Vitro Drug Release

The release medium was prepared by mixing 40% ethanol and 1% sodium lauryl sulfate (SLS). A total of 100 mL of release medium and 2 mL of NLC samples or silymarin solution (15 mg/mL) were placed in a dialysis bag and incubated in a shaker at 100 rpm and 37°C. Samples were collected at 2, 4, 6, 8, and 24 hours, and released silymarin was quantified by UV spectrophotometry. All experiments were performed in triplicate. Finally, a graph of cumulative release percentage over time (h) was plotted for each sample.

3.12. In Vitro Determination of Sun Protection Effect (SPF)

The SPF of the formulations was determined by evaluating the spectral transmittance of UVR through Transpore 3M tape with and without sunscreen, a method originally proposed by Diffey and Robson. Briefly, freshly prepared samples were dotted onto the tape placed on a quartz slide and spread evenly using a circular motion (2 mg/cm^2). Transmission values were then recorded at wavelengths between 290 and 400 nm. The sun protection factors of the formulations were calculated using the following equation (21, 22):

$$\mathrm{SPF} = \frac{\int_{290}^{400} E(\lambda).S(\lambda).\mathrm{d}\lambda}{\int_{290}^{400} E(\lambda).S(\lambda).T(\lambda).\mathrm{d}\lambda}$$

where E(λ) is the spectral irradiance of terrestrial sunlight at λ, S(λ) is the erythemal action spectrum at λ, and T(λ) is the spectral transmittance of the sample at λ. To validate the SPF values, a commercial sunscreen formulation (Sunscreen cream SPF30, Ardene Sun) was used as a positive control. This test was performed for each formulation in triplicate.

3.13. Stability Studies

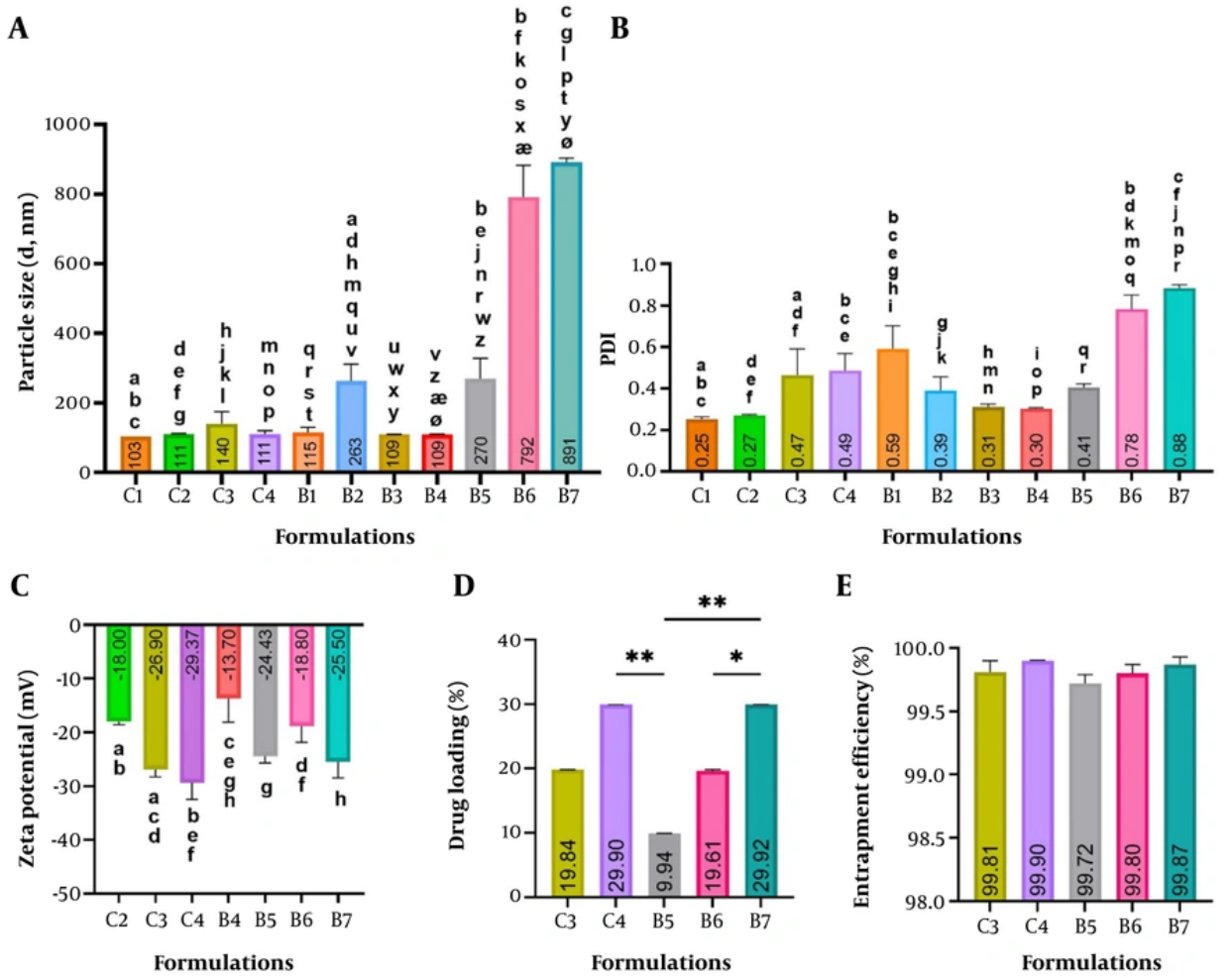

Figure 1. Particle size (A), PDI (B), zeta potential (C), drug loading (D), and drug entrapment efficiency (E) of different NLC formulations. Data are mean ± SD, n = 3. Identical letters at the top of columns represent significant differences between groups ($P < 0.05$); *: $P \leq 0.05$; **: $P \leq 0.01$.

Stability studies were performed by storing samples at ambient temperature and measuring particle size at time zero and after 2 weeks, 4 weeks, and 3 months, as previously described.

3.14. Statistical Analysis

Statistical analyses were performed using GraphPad Prism version 9 (GraphPad Software Inc., CA, USA). Average particle size, PDI, zeta potential, and SPF values were analyzed using one-way analysis of variance (ANOVA), followed by Tukey's post hoc test. For EE (%) data, ANOVA was performed without a post hoc test because of minimal intergroup variability. DL (%) data that did not meet normality assumptions were analyzed nonparametrically using the Kruskal-Wallis test and the post hoc Dunn test. For all tests, a P value of less than 0.05 was considered significant. Experiments were performed in triplicate (n = 3), and data are presented as mean ± standard deviation. The normality of residuals was assessed using Q-Q plots and the D'Agostino-Pearson omnibus test. Homogeneity of variance was assessed using the Brown-Forsythe test (Table1 in Supplementary File).

4. Results

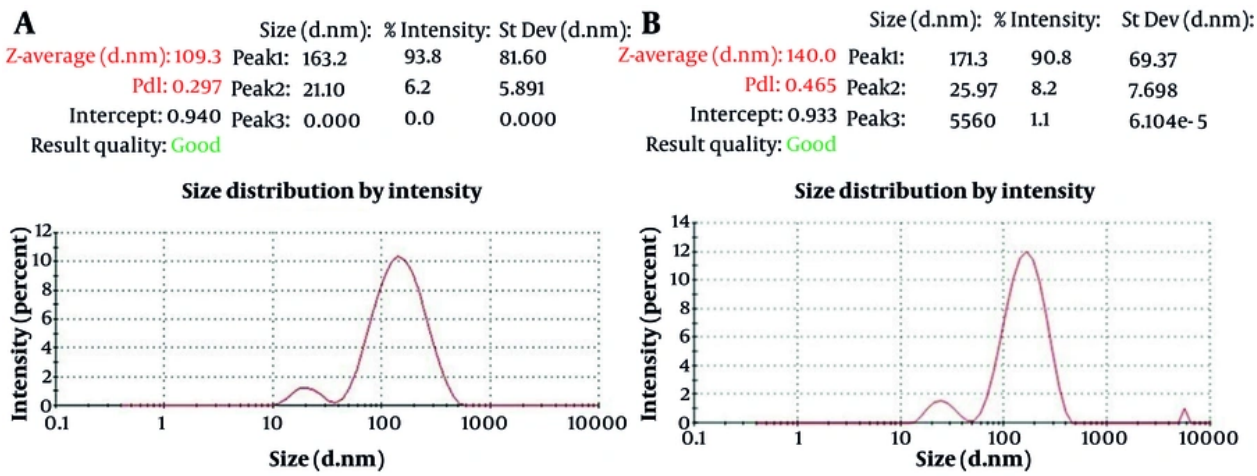

Figure 2. Size and size distribution curves of B4 (A) and C2 (B) formulations.

4.1. Particle Size and Zeta Potential

In this study, five NLC and six silymarin-NLC formulations containing different proportions of solid and liquid lipids and different amounts of silymarin were prepared (Table 1). The particle size and polydispersity index of the formulations are summarized in Figure 1A and Figure 1B, respectively.

As shown in Figure 1A, the mean size of formulations C1-C4 ranged from 102.9 nm (C1) to 140.0 nm (C3), whereas the mean size of formulations B1-B7 ranged from 108.8 nm (B3) to 890.8 nm (B7). The PDI ranges of formulations C1-C4 and B1-B7 were 0.25 (C1) to 0.49 (C4) and 0.30 (B4) to 0.88 (B7), respectively (Figure 1B). Figure 2 shows the particle size and PDI of two optimal blank formulations, B4 and C2. The particle size distributions were bimodal, with a dominant NLC population and a secondary peak with a smaller mean diameter (~21 - 26 nm) accounting for approximately 6 - 8% of the total intensity. This minor population is most likely associated with surfactant micelles or mixed micellar aggregates, which are known to appear at higher total lipid and surfactant concentrations (15% w/w). A very small third peak with a large size (~5.5 μm) observed in B4 may correspond to occasional aggregates or dust particles.

As shown in Figure 1, there was no significant difference in size or PDI between B4 and C2. However, increasing drug concentration led to a dramatic and significant rise in particle size and PDI in BW-containing formulations, whereas the changes in CP-containing formulations were not significant. Several studies have shown that increasing drug concentration increases the mean particle size, likely because of drug entrapment within the lipid matrix or on the particle surface (11).

Zeta potential measures the electrical charge on nanoparticles and indicates their tendency to aggregate. As illustrated in Figure 1C, drug loading increased the negative charge in formulations C2 and B4, and this change was significant in all cases except for B6. Values less than -20 mV and greater than +20 mV are considered stable. As shown in Figure 1, the zeta potentials of all silymarin-NLCs were more than or around -20 mV.

4.2. Drug Loading and Entrapment Efficiency

The results of drug loading (DL) and drug entrapment efficiency (EE) are presented in Figure 1D and Figure 1E. All formulations achieved an EE (%) above 99.7%. No significant difference in %EE was observed among the groups. Increasing the silymarin concentration from 1.5% to 4% (in formulations B5 to B7) resulted in a significant increase in DL from 9.94% to 29.9%. Similarly, increasing the silymarin concentration from 3% in C3 to 4% in C4 increased the loading percentage from 19.86% to 29.9%.

4.3. FTIR Analysis

Infrared spectra of pure silymarin and NLC formulations are shown in Figure 3. The FTIR spectrum of pure silymarin showed a broad O-H stretching band

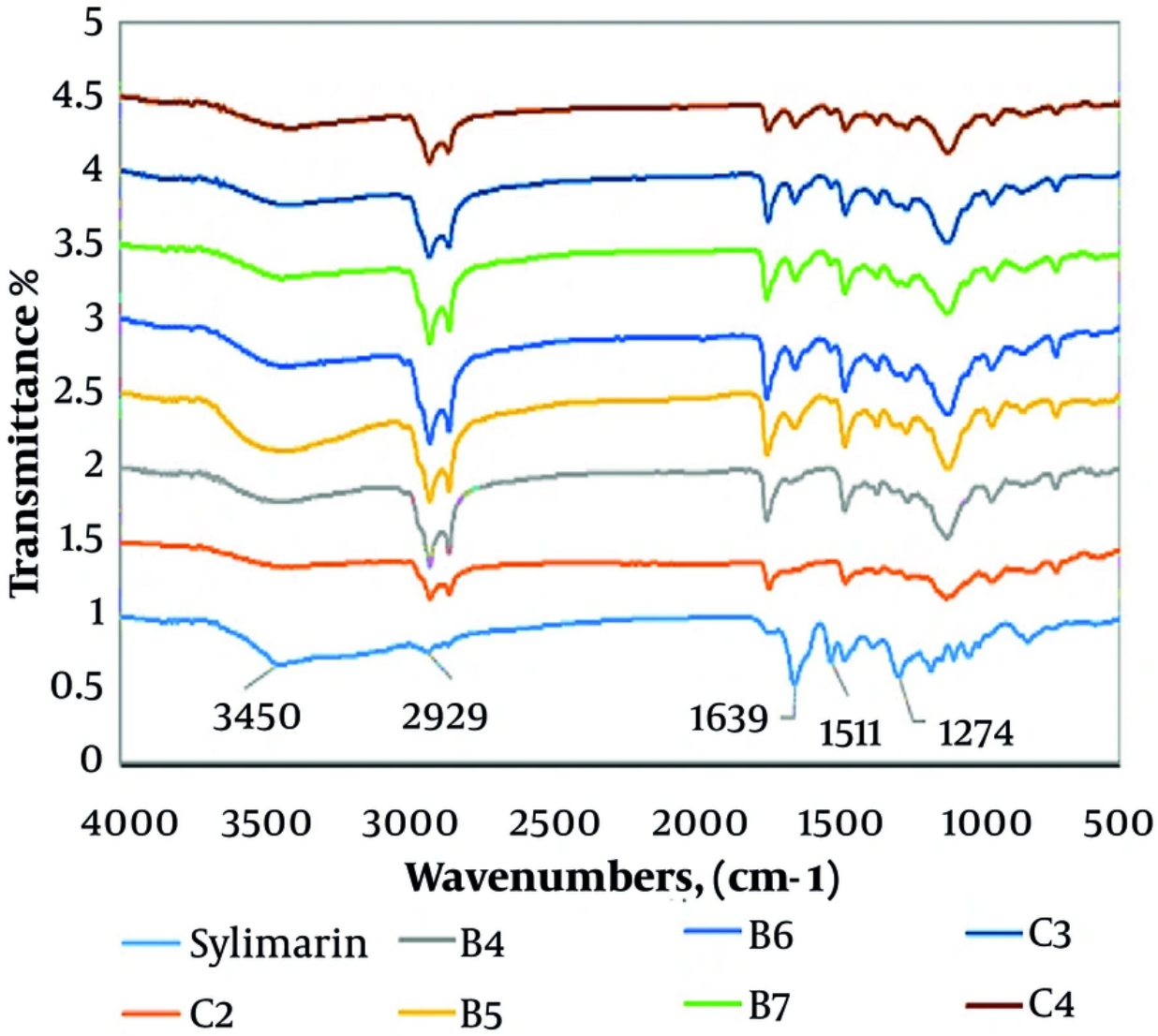

Figure 3. FTIR spectra of silymarin and silymarin-NLC formulations.

at 3450 cm^{-1}, strong aliphatic/aromatic C-H stretching at 2929 and 2850 cm^{-1}, a characteristic flavonolignan C=O band at 1635 cm^{-1}, an aromatic C=C stretching band at 1511 cm^{-1}, and a C-O stretching vibration at 1274 cm^{-1} (23, 24). The FTIR spectra of the silymarin-loaded NLC formulations showed the same characteristic peaks, particularly those around 1639 cm^{-1} and 1511 cm^{-1}, with only minor shifts or broadening. This finding can be attributed to physical interactions, such as hydrogen bonding or molecular dispersion of silymarin within the lipid matrix, without major chemical interaction. In contrast, these diagnostic silymarin bands were absent in the blank carriers (C2 and B4), confirming that the observed peaks in the drug-loaded formulations originated from silymarin.

4.4. DSC Analysis

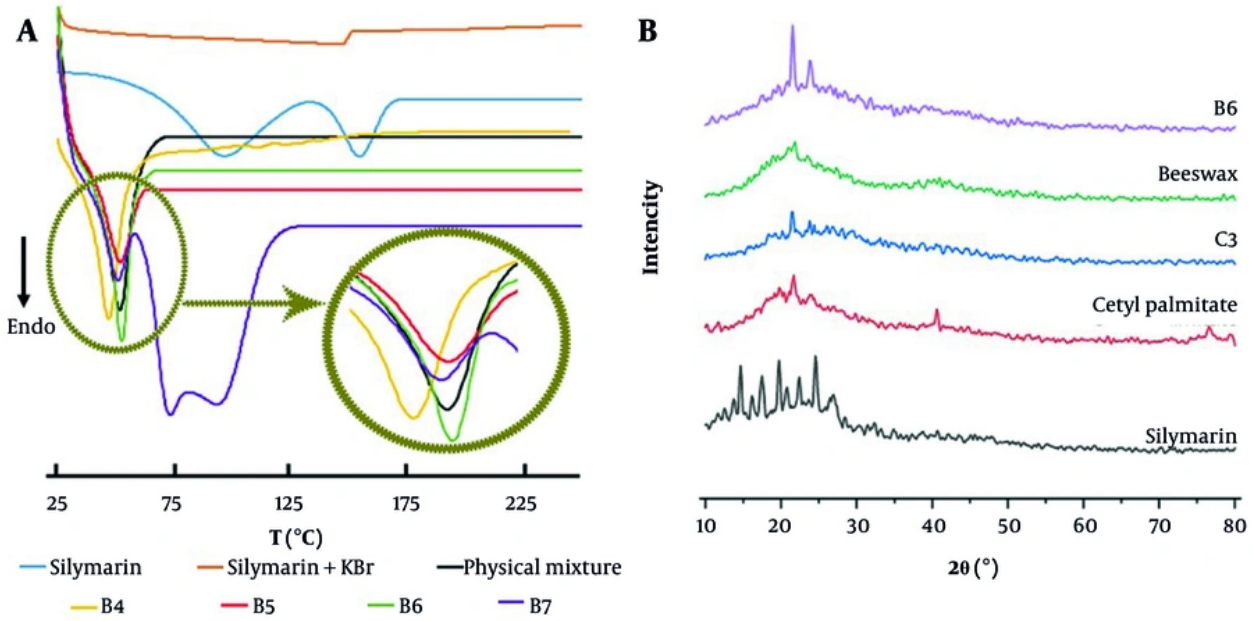

Figure 4. (A) DSC thermograms of silymarin, a physical mixture consisting of silymarin, beeswax, oleic acid, Tween 80, a geometrical mixture of silymarin + KBr, and NLC formulations containing beeswax (B4-B7); (B) XRD diffractograms of silymarin, cetyl palmitate, beeswax, and silymarin-NLC formulations containing 3% drug (C3 and B6).

DSC analysis was used to identify changes in thermal transitions. The DSC thermogram of pure silymarin (Figure 4A) showed two broad peaks at 96.15°C and 154.93°C. The initial peak likely corresponds to residual moisture in the sample, whereas the latter indicates the drug melting point. The silymarin + KBr mixture showed a minimal peak because of the dilution of silymarin in KBr. Silymarin-NLC formulations (B5-B7) presented an endothermic peak for BW melting (62 - 64°C) without the silymarin peak (154.93°C). This implies that crystalline silymarin was effectively converted to an amorphous or soluble state, or that the drug was well integrated into the melted lipid matrix (15). Two broad peaks in the B7 formulation (72 - 92°C) were associated with the moisture content of the formulation.

4.5. XRD Analysis

The X-ray diffraction spectra of pure silymarin, CP, BW, and two silymarin-NLC formulations containing 3% drug (C3 and B6) are shown in Figure 4B. The diffraction pattern of plain silymarin exhibited sharp and intense peaks at 2θ of 13.75, 14.65, 16.15, 17.35, 19.75, 20.80, 22.45, 24.55, and 26.95°, reflecting the crystalline nature of silymarin (25). In accordance with prior studies, the diffractogram of CP revealed major peaks at 2θ of 21.5, 23.8, and 40.6° (26, 27), and the diffractogram of BW showed main peaks at 2θ of 21.5° and 24° (28, 29). In the XRD pattern of C3, two peaks at 2θ of 21.5 and 23.8° were observed, which could be related to CP. The XRD pattern of B6 similarly showed two peaks at 2θ values corresponding to those in the BW profile, but with increased intensity. The characteristic peaks of plain silymarin were not identifiable in the diffractograms of C3 and B6, suggesting decreased peak intensity or peak broadening, consistent with reduced drug crystallinity. It is plausible that silymarin exists in an amorphous state or is uniformly dispersed within the lipid matrix (25). These results were consistent with the findings on entrapment efficiency and DSC analysis.

4.6. Rheological Studies

Rheological studies are essential for products intended for skin application. These products must be easily spreadable and non-dripping. The rheograms of B4-B7 and C2-C4 NLC formulations, along with a commercial sunscreen, are shown in Figure 5. Although B4 and C2 were colloidal dispersions and the remaining NLCs were semisolids, all formulations showed a time-dependent reduction in viscosity, indicating increased

Table 2. Viscosity of NLC Formulations and Commercial Sunscreen at Selected Shear Rates

Formulations	Viscosity at 51.66 s^{-1} (Pa·s),		Viscosity at 155.16 s^{-1} (Pa·s)		Viscosity at 300 s^{-1}(Pa·s)	
	Up Sweep	Down Sweep	Up Sweep	Down Sweep	Up Sweep	Down Sweep
B4	1.61	1.60	0.51	0.51	0.28	0.28
B5	2.06	1.90	0.82	0.75	0.49	0.49
B6	3.10	1.90	0.79	0.64	0.39	0.39
B7	3.20	2.28	1.01	0.84	0.56	0.55
C2	1.22	1.20	0.48	0.45	0.25	0.25
C3	2.35	1.38	0.70	0.51	0.33	0.33
C4	3.28	1.93	1.50	0.99	0.88	0.87
Commercial sunscreen (SPF30)	2.91	1.44	0.92	0.68	0.49	0.49

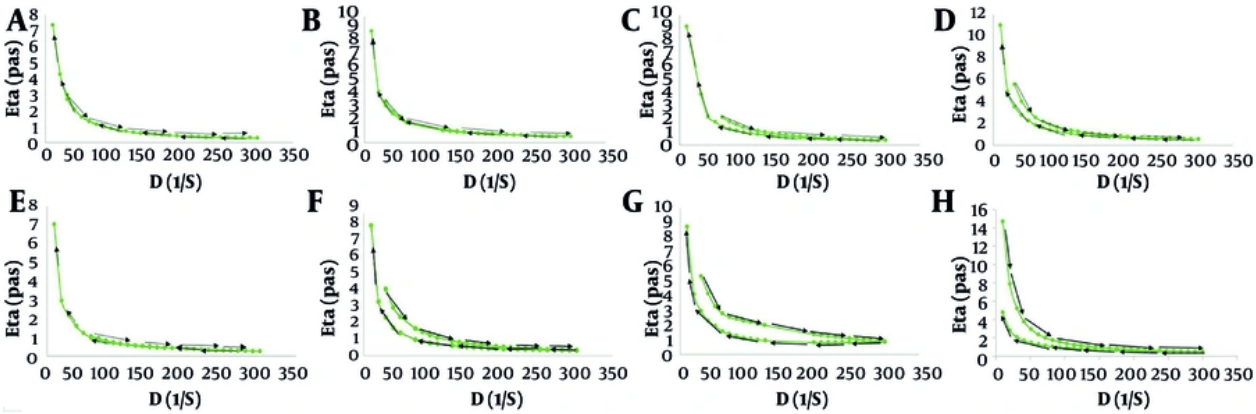

Figure 5. Rheograms of NLC formulations: (A) B4, (B) B5, (C) B6, (D) B7, (E) C2, (F) C3, (G) C4, and (H) a commercial sunscreen cream SPF30.

flowability. This behavior, reflecting their non-Newtonian, shear-thinning, and pseudoplastic properties, was also observed in the commercial sunscreen. Vergilio et al. conducted rheological analysis of seven commercial sunscreens available in the Brazilian market. The analyzed sunscreens were categorized as non-Newtonian fluids and demonstrated pseudoplastic characteristics. The authors considered this behavior important for topical products because viscosity decreases with increasing shear rate. Pseudoplastic systems can achieve smooth flow, resulting in improved dispersion during application and formation of a uniform layer on the skin surface (30). In addition, B6, B7, C3, and C4 showed thixotropic behavior suitable for sunscreen products. In this case, with increasing shear force, the network structure of the formulation breaks down, enabling proper removal of the product from the container, facilitating spreading, and promoting photoprotection ability. This behavior was also observed in the commercial sunscreen tested (Figure 5H). Comparison of the viscosity values of the NLCs formulated in this study with those of the commercial sunscreens examined in this study (Table 2) and in the study by Vergilio et al. (30) shows that the viscosity of the NLCs falls within the range of viscosities reported for the commercial samples.

4.7. In Vitro Release Studies

An in vitro release study of silymarin and silymarin-NLC formulations was conducted for 24 hours, and the release profiles are presented in Figure 6. All formulations showed an initially rapid release during the first 8 hours. Based on many previous studies, drug release from NLCs can be divided into two phases: an initial burst release followed by sustained drug release. This outcome is attributed to events during NLC preparation. The drug initially distributes into both lipid and aqueous phases at high temperature. Upon

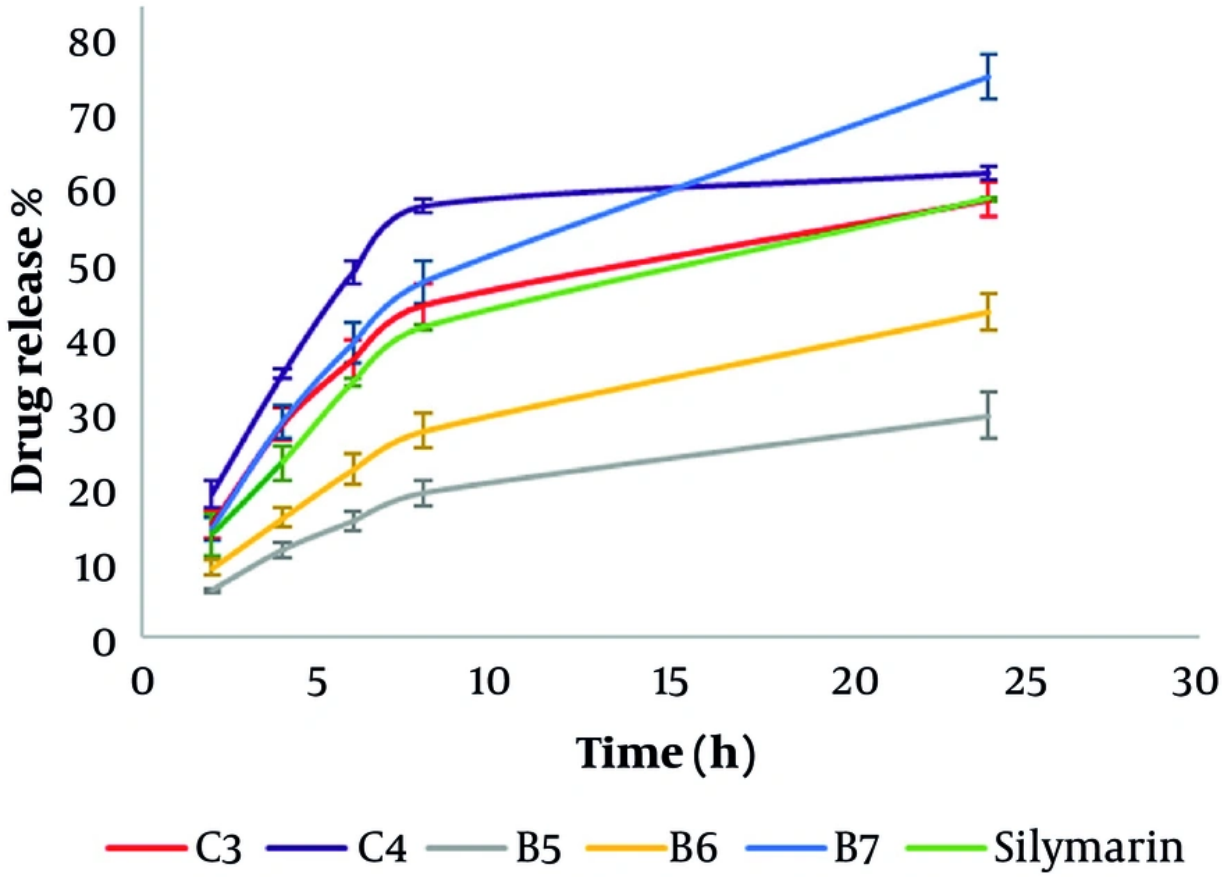

Figure 6. in vitro release study of silymarin and silymarin-NLC formulations. Data are expressed as mean ± SD, n = 3.

cooling, the drug predominantly re-enters the lipid phase, whereas some remains on the particle surface. The accumulated drug on the nanoparticle surface triggers the initial burst-release phase. The second phase results from drug diffusion from the lipid core or matrix degradation (31, 32).

The burst-release rate in C3, C4, and B7 was higher than that of bare silymarin and the other formulations. Enhanced release of poorly soluble drugs from NLC formulations compared with free drugs has been reported in earlier studies and has been used to improve their pharmacokinetic profile (33). Furthermore, comparison of formulations with the same drug concentration (C3 vs. B6 and C4 vs. B7) showed that the type of solid lipid significantly affected drug release. Formulations containing CP had a higher drug-release rate than formulations containing BW. Controlling drug release is an important goal in sunscreen formulations; according to these results, BW is a more effective solid lipid than CP for this purpose. Lipids with shorter fatty acid chains are more permeable and degrade faster than those with longer chains. BW is a heterogeneous mixture of fatty acids of different lengths, some of which are longer than CP. In addition, smaller particle sizes in NLCs lead to quicker drug release because of the larger surface area (32). As previously mentioned, formulations containing CP had smaller particle sizes than formulations containing BW. This finding is consistent with previous studies reporting that the drug-release rate increases with increasing DL and EE (32).

4.8. In Vitro Determination of Sun Protection Effect

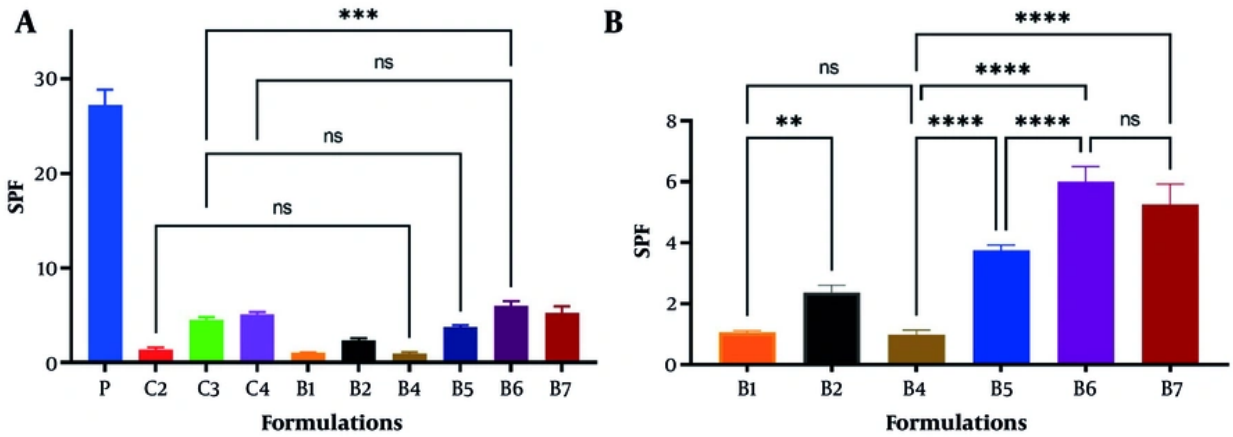

Figure 7. The SPF values of NLC formulations. (A) A statistical analysis comparing formulations that contain cetyl palmitate with those that include beeswax. (B) A statistical analysis of formulations that contain beeswax. P: a sunscreen formulation with SPF value of 30 (Ardene Sun), used as a positive control; data are mean ± SD, n = 3; ns: P > 0.05; *: P ≤ 0.05; **: P ≤ 0.01; ***: P ≤ 0.001; ****: P ≤ 0.0001.

As illustrated in Figure 7A, when comparing CP-containing NLCs with those containing BW, the SPF values of the two drug-free formulations (C2 and B4) were not significantly different. However, the SPF value of B6 was considerably greater than that of C3 (p-value > 0.001), although both contained 3% silymarin. In addition, no significant difference was observed between the SPF value of C3 and B5 (1.5% silymarin). Formulations containing BW and silymarin appear to provide better sun protection than formulations containing CP and silymarin. Although the achieved SPF values (3.76 - 6.01) confirm the UV absorption properties of silymarin, they remain considerably below clinically relevant SPF levels.

The commercial sunscreen cream (Ardene Sun, labeled SPF 30) was tested to validate the accuracy of the SPF method. It yielded an SPF value of 27.20 ± 1.63, which fell within the 95% confidence interval (23.15 - 31.25) of the labeled SPF. Minor deviations between in vitro spectrophotometric measurements and labeled SPF values determined by in vivo methods are expected because of methodological differences.

Comparison of SPF values between B1 and B4 indicated that increasing lipid content did not influence the SPF value (Figure 7B. Furthermore, increasing the drug concentration to 3% resulted in a notable rise in SPF values. Conversely, increasing the drug concentration from 3% (in C3 and B6) to 4% (in C4 and B7) did not yield a significant change in the SPF value. Because the SPF values were obtained from freshly prepared samples, the likelihood of aggregation was low. The lack of an increase in SPF from 3% to 4% silymarin probably reflects a change in drug distribution within the NLCs: at higher loading, a portion of the silymarin may form clusters near the particle surface rather than remaining molecularly dispersed. This interpretation is consistent with the faster release rate observed for B7 compared with B6 and for C4 compared with C3. Overall, the highest SPF value was found in B6 (6.01 ± 0.40). Rencber et al. used Precirol ATO 5, Tween 80, and Tween 20 to develop NLC by the high-shear homogenization method. The SPF value of the formulation with 2% silymarin was 3.88 ± 0.23 (8). In this study, the SPF value of B5 was 3.76 ± 0.14.

4.9. Stability Studies

Formulations B5-B7 showed acceptable particle size and polydispersity index (PDI) during the initial weeks. However, after three months of storage, all three formulations had a PDI of 1.0, indicating a complete loss of colloidal stability and substantial particle aggregation (Table 3). This suggests that the formulations failed and are not suitable for long-term storage in their current state. In the present study, increasing the total lipid and surfactant content to 15% (w/w) enhanced drug loading in the formulations but may also have led to greater particle aggregation during storage. Notably, particle size increased significantly in silymarin-loaded formulations compared with empty NLCs (B4), indicating that both drug incorporation and

Table 3. Stability Studies of Silymarin-NLC Formulations

Formulation Code	Zero-time		Two Weeks		Four Weeks		Three Months	
	Average Size (nm)	PDI	Average Size (nm)	Two Weeks PDI	Average Size (nm)	Four Weeks PDI	Average Size (nm)	Three Months PDI
B4	109.3	0.30	108.7	0.27	160.8	0.41	216	0.43
B5	269.6	0.40	284.7	0.50	610.6	0.63	2327	1.00
B6	791.8	0.78	370.0	0.59	569.7	0.60	2504	1.00
B7	890.8	0.88	799.0	0.70	689.6	0.72	2303	1.00

elevated excipient levels may contribute to instability. This observation aligns with previous studies reporting size increases in formulations with high silymarin content and lipid percentages, even at the initial preparation stage (8). Therefore, although the developed system shows potential as a silymarin carrier, further optimization, such as increasing surface charge or steric stabilization, is necessary to improve long-term stability. Further studies, including stability testing at refrigerated temperatures and longer-term testing, are also needed.

5. Discussion

In this research, NLCs were developed using melt emulsification and high-shear homogenization, yielding formulations with acceptable initial particle size and size distribution at time zero. However, formulations with higher drug loading did not maintain long-term colloidal stability. The observed aggregation and complete loss of homogeneity after three months suggest that these systems require substantial reformulation to improve stability.

To protect the skin from ultraviolet (UV) radiation, a large amount of silymarin needed to be incorporated into the NLCs. This amount was substantially higher than that used in NLCs prepared for other purposes in previous studies. Previous studies developed NLCs with silymarin concentrations of 2 mg/mL (10, 13), 4 mg/mL (14), and 10 mg/mL (15) for different skin treatments. Only one recent study used a higher concentration of silymarin (2%), combined with zinc oxide in NLCs, to evaluate its protective effects against UV-induced damage (8). Drug loading and entrapment studies confirmed that silymarin was successfully entrapped in the NLCs with high efficiency. The DSC, XRD, and FTIR analyses also supported this conclusion. Moreover, formulations containing BW showed more controlled release and relatively higher SPF values than those containing CP. This finding is noteworthy because beeswax is a naturally derived, inexpensive, and widely available lipid.

The relatively low SPF results ($\leq$ 6) in this study indicate the limited inherent absorption capacity of silymarin compared with commercial filters. Natural compounds usually exhibit moderate SPF; however, their use in sunscreens can reduce harmful synthetic ingredients, thereby improving product safety. Thus, achieving high SPF values without conventional UV filters remains impractical (34). Nevertheless, silymarin is currently of great interest in topical formulations because of its antioxidant, anti-inflammatory, and anti-photoaging properties. Therefore, future research will focus on co-formulation with existing UV filters to investigate potential synergistic effects on increasing SPF and overall photoprotection. Without such co-formulation, the present NLCs cannot be regarded as clinically effective sunscreen products. Moreover, the lack of biocompatibility assessments, including cytotoxicity, irritation, sensitization, and phototoxicity evaluations, is a significant limitation of the current study, as these tests were planned to be performed after co-formulation with UV filters for the final product.

Supplementary Material

Supplementary material(s) is available here [To read supplementary materials, please refer to the journal website and open PDF/HTML].

Footnotes

AI Use Disclosure: The authors declare that no generative AI tools were used in the creation of this article.

Authors' Contribution: N. A. prepared the NLCs, conducted the characterization experiments, and collected the data. A. G. designed and supervised the development and characterization of the NLCs and analyzed the data. A. T. designed and supervised the experiments for determining the sun protection effect. M. A. contributed to data interpretation and manuscript drafting. S. J. conceived the project, performed the

statistical analysis, contributed to manuscript writing, and critically revised the manuscript.

Conflict of Interests Statement: The authors declare no conflict of interest.

Data Availability: The dataset presented in the study is available on request from the corresponding author during submission or after publication.

Ethical Approval: The study received ethical approval from the Ethics Committee of Zanjan University of Medical Sciences (IR.ZUMS.REC.1397.109)

Funding/Support: This research received financial support from Zanjan University of Medical Sciences, grant number A-12 - 851 - 7 (https://old.zums.ac.ir/rds/index.php?sid=1&slc_lang=fa). The authors wish to acknowledge Goldaru Pharmaceutical Co., Iran, for the gift sample of silymarin.

References

1. Saadh MJ, Jain V, Rekha MM, Pathak PK, Ahmed HM, Satyam Naidu K, et al. Recent advancement on nanotechnology and natural compounds for skin UV protection: a review. *Int J Environ Sci Te*. 2025;**22**(13):13223-44. https://doi.org/10.1007/s13762-025-06589-w.
2. Hegde AR, Kunder MU, Narayanaswamy M, Murugesan S, Furtado SC, Veerabhadraiah BB, et al. Advancements in sunscreen formulations: integrating polyphenolic nanocarriers and nanotechnology for enhanced UV protection. *Environ Sci Pollut Res Int*. 2024;**31**(26):38061-82. [PubMed ID: 38806984]. https://doi.org/10.1007/s11356-024-33712-0.
3. Fonseca M, Rehman M, Soares R, Fonte P. The impact of flavonoid-loaded nanoparticles in the UV protection and safety profile of topical sunscreens. *Biomolecules*. 2023;**13**(3):493. [PubMed ID: 36979428]. [PubMed Central ID: PMC10046639]. https://doi.org/10.3390/biom13030493.
4. Katiyar SK, Mantena SK, Meeran SM. Silymarin protects epidermal keratinocytes from ultraviolet radiation-induced apoptosis and DNA damage by nucleotide excision repair mechanism. *PLoS One*. 2011;**6**(6). e21410. [PubMed ID: 21731736]. [PubMed Central ID: PMC3120878]. https://doi.org/10.1371/journal.pone.0021410.
5. Rajnochová Svobodová A, Gabrielová E, Michaelides L, Kosina P, Ryšavá A, Ulrichová J, et al. UVA-photoprotective potential of silymarin and silybin. *Arch Dermatol Res*. 2018;**310**(5):413-24. [PubMed ID: 29564550]. https://doi.org/10.1007/s00403-018-1828-6.
6. Milutinov J, Pavlović N, Ćirin D, Atanacković Krstonošić M, Krstonošić V. The potential of natural compounds in UV protection products. *Molecules*. 2024;**29**(22):5409. [PubMed ID: 39598798]. [PubMed Central ID: PMC11597743]. https://doi.org/10.3390/molecules29225409.
7. Erdoğan Ü, Gökçe EH, Muhammed MT, Önem E, Erten AA, Süleymanoğlu B. Milk thistle extracts could enhance the UV-protection efficiency and stability of mineral filters in sunscreen formulations. *J Photochem Photobiol A Chem*. 2024;**450**. 115460. https://doi.org/10.1016/j.jphotochem.2024.115460.
8. Rencber S, Aydin HH, Gultekin HE, Aydin-Kose F, Senyigit Z. Silymarin and zinc oxide loaded semi-solid lipid nanoparticle formulations against UV-induced skin damage. *J Dispers Sci Technol*. 2025;**47**(2):218-235. https://doi.org/10.1080/01932691.2025.2514806.
9. Di Costanzo A, Angelico R. Formulation strategies for enhancing the bioavailability of silymarin: the state of the art. *Molecules*. 2019;**24**(11):2155. [PubMed ID: 31181687]. [PubMed Central ID: PMC6600503]. https://doi.org/10.3390/molecules24112155.
10. Singh P, Singh M, Kanoujia J, Arya M, Saraf SK, Saraf SA. Process optimization and photostability of silymarin nanostructured lipid carriers: effect on UV-irradiated rat skin and SK-MEL 2 cell line. *Drug Deliv Transl Res*. 2016;**6**(5):597-609. [PubMed ID: 27431400]. https://doi.org/10.1007/s13346-016-0317-8.
11. Subramaniam B, Siddik ZH, Nagoor NH. Optimization of nanostructured lipid carriers: understanding the types, designs, and parameters in the process of formulations. *J Nanopart Res*. 2020;**22**(6). 141. https://doi.org/10.1007/s11051-020-04848-0.
12. Chavda VP, Acharya D, Hala V, Daware S, Vora LK. Sunscreens: a comprehensive review with the application of nanotechnology. *J Drug Deliv Sci Technol*. 2023;**86**. 104720. https://doi.org/10.1016/j.jddst.2023.104720.
13. Singh P, Arya M, Kanoujia J, Singh M, Gupta KP, Saraf SA. Design of topical nanostructured lipid carrier of silymarin and its effect on 7, 12-dimethylbenz[a]anthracene (DMBA) induced cellular differentiation in mouse skin. *RSC Adv*. 2016;**6**(88):84965-77. https://doi.org/10.1039/C6RA20231D.
14. Iqbal B, Ali J, Ganguli M, Mishra S, Baboota S. Silymarin-loaded nanostructured lipid carrier gel for the treatment of skin cancer. *Nanomedicine*. 2019;**14**(9):1077-93. [PubMed ID: 31050580]. https://doi.org/10.2217/nnm-2018-0235.
15. Momin F, Kevlani V, Rawal S, Patel R, Acharya S, Shah S. Antipsoriatic effect of silymarin NLCs based gel: in vitro and in vivo activity. *AAPS PharmSciTech*. 2024;**25**(7). 195. [PubMed ID: 39168904]. https://doi.org/10.1208/s12249-024-02910-x.
16. Shangguan M, Qi J, Lu Y, Wu W. Comparison of the oral bioavailability of silymarin-loaded lipid nanoparticles with their artificial lipolysate counterparts: implications on the contribution of integral structure. *Int J Pharm*. 2015;**489**(1):195-202. [PubMed ID: 25956049]. https://doi.org/10.1016/j.ijpharm.2015.05.005.
17. Chaudhary S, Garg T, Murthy RSR, Rath G, Goyal AK. Development, optimization and evaluation of long chain nanolipid carrier for hepatic delivery of silymarin through lymphatic transport pathway. *Int J Pharm*. 2015;**485**(1):108-21. [PubMed ID: 25735668]. https://doi.org/10.1016/j.ijpharm.2015.02.070.
18. Shangguan M, Lu Y, Qi J, Han J, Tian Z, Xie Y, et al. Binary lipids-based nanostructured lipid carriers for improved oral bioavailability of silymarin. *J Biomater Appl*. 2014;**28**(6):887-96. [PubMed ID: 24008629]. https://doi.org/10.1177/0885328213485141.
19. Cengiz M, Kutlu HM, Burukoglu DD, Ayhancı A. A comparative study on the therapeutic effects of silymarin and silymarin-loaded solid lipid nanoparticles on D-GaIN/TNF-α-induced liver damage in Balb/c mice. *Food Chem Toxicol*. 2015;**77**:93-100. [PubMed ID: 25544390]. https://doi.org/10.1016/j.fct.2014.12.011.
20. Basso J, Mendes M, Cova T, Sousa J, Pais A, Fortuna A, et al. A stepwise framework for the systematic development of lipid nanoparticles. *Biomolecules*. 2022;**12**(2):223. [PubMed ID: 35204723]. [PubMed Central ID: PMC8961617]. https://doi.org/10.3390/biom12020223.
21. Draghici-Popa AM, Buliga DI, Popa I, Tomas ST, Stan R, Boscornea AC. Cosmetic products with potential photoprotective effects based on natural compounds extracted from waste of the winemaking industry. *Molecules*. 2024;**29**(12):2775. [PubMed ID: 38930846]. [PubMed Central ID: PMC11206142]. https://doi.org/10.3390/molecules29122775.
22. Sharma B, Chauhan I. in vitro and in vivo evaluation of sunscreen formulations containing nanolipid carriers. *Curr Cosmet Sci*.

2022;**1**(2). e190822207741. https://doi.org/10.2174/2666779701666220819144607.

23. Zhu Y, Wang M, Zhang Y, Zeng J, Omari-Siaw E, Yu J, et al. in vitro release and bioavailability of silybin from micelle-templated porous calcium phosphate microparticles. *AAPS PharmSciTech*. 2016;**17**(5):1232-9. [PubMed ID: 26669888]. https://doi.org/10.1208/s12249-015-0460-4.
24. Madiyar F, Suskavcevic L, Daugherty K, Weldon A, Ghate S, O'Brien T, et al. Optimizing production, characterization, and in vitro behavior of silymarin-Eudragit electrosprayed fiber for anti-inflammatory effects: a chemical study. *Bioengineering*. 2024;**11**(9):864. [PubMed ID: 39329606]. [PubMed Central ID: PMC11428713]. https://doi.org/10.3390/bioengineering11090864.
25. Sherikar A, Siddique MUM, More M, Goyal SN, Milivojevic M, Alkahtani S, et al. Preparation and evaluation of silymarin-loaded solid eutectic for enhanced anti-inflammatory, hepatoprotective effect: in vitro-in vivo prospect. *Oxid Med Cell Longev*. 2021;**2021**(1). 1818538. [PubMed ID: 34804361]. [PubMed Central ID: PMC8598371]. https://doi.org/10.1155/2021/1818538.
26. Sadegh Malvajerd S, Azadi A, Izadi Z, Kurd M, Dara T, Dibaei M, et al. Brain delivery of curcumin using solid lipid nanoparticles and nanostructured lipid carriers: preparation, optimization, and pharmacokinetic evaluation. *ACS Chem Neurosci*. 2019;**10**(1):728-39. [PubMed ID: 30335941]. https://doi.org/10.1021/acschemneuro.8b00510.
27. Pornputtapitak W, Thiangjit Y, Tantirungrotechai Y. Effect of functional groups in lipid molecules on the stability of nanostructured lipid carriers: experimental and computational investigations. *ACS Omega*. 2024;**9**(9):11012-24. [PubMed ID: 38463339]. [PubMed Central ID: PMC10918666]. https://doi.org/10.1021/acsomega.4c00685.
28. Ambrosi M, Raudino M, Pieraccini G, Corti C, Tenorio-Alfonso A, Martínez I. Understanding the formation of efflorescence on beeswax models housed at the Natural History Museum of Florence. *J Cult Herit*. 2023;**62**:143-50. https://doi.org/10.1016/j.culher.2023.05.023.
29. Dantas IL, Bastos KTS, Machado M, Galvão JG, Lima AD, Gonsalves JKMC, et al. Influence of stearic acid and beeswax as solid lipid matrix of lipid nanoparticles containing tacrolimus. *J Therm Anal Calorim*. 2018;**132**(3):1557-66. https://doi.org/10.1007/s10973-018-7072-7.
30. Vergilio MM, de Freitas ACP, da Rocha-Filho PA. Comparative sensory and instrumental analyses and principal components of commercial sunscreens. *J Cosmet Dermatol*. 2022;**21**(2):729-39. [PubMed ID: 33786956]. https://doi.org/10.1111/jocd.14113.
31. Czajkowska-Kośnik A, Szymańska E, Czarnomysy R, Jacyna J, Markuszewski M, Basa A, et al. Nanostructured lipid carriers engineered as topical delivery of etodolac: optimization and cytotoxicity studies. *Materials (Basel)*. 2021;**14**(3):596. [PubMed ID: 33514018]. [PubMed Central ID: PMC7866147]. https://doi.org/10.3390/ma14030596.
32. Haider M, Abdin SM, Kamal L, Orive G. Nanostructured lipid carriers for delivery of chemotherapeutics: a review. *Pharmaceutics*. 2020;**12**(3):288. [PubMed ID: 32210127]. [PubMed Central ID: PMC7151211]. https://doi.org/10.3390/pharmaceutics12030288.
33. Poonia N, Kharb R, Lather V, Pandita D. Nanostructured lipid carriers: versatile oral delivery vehicle. *Future Sci OA*. 2016;**2**(3). FSO135. [PubMed ID: 28031979]. [PubMed Central ID: PMC5137980]. https://doi.org/10.4155/fsoa-2016-0030.
34. Morocho-Jácome AL, Freire TB, de Oliveira AC, de Almeida TS, Rosado C, Velasco MVR, et al. in vivo SPF from multifunctional sunscreen systems developed with natural compounds-A review. *J Cosmet Dermatol*. 2021;**20**(3):729-37. [PubMed ID: 32649016]. https://doi.org/10.1111/jocd.13609.